The Study of Flow and Reaction Rates in Turbulent Flames

R. P. BARBOR, J. D. LARKIN, H. E. VON ROSENBERG, and C. W. SHIPMAN University of Delaware, Newark, Delaware

It is proposed that measurements of reaction rate as a function of position within turbulent flames be the basis of an approach to the problem of turbulent-flame propagation. As a test of the method, measurements of static pressure, impact pressure, and chemical composition were made at several positions within the burning zones of two simulated ramjet combustion chambers. From these measurements a complete mapping of compositions, velocity components, densities, and static pressures could be carried out. By calculation of the appropriate derivatives of the latter quantities, the differential form of the equation of continuity for the species desired could be solved for net reaction rate as a function of position, turbulent diffusion being neglected. By a similar technique the equation of momentum was used to obtain eddy viscosities. The latter results were used to estimate the effect of turbulent diffusion by assuming a turbulent Schmidt number of unity.

It is concluded that the method of attack used is a reasonable approach to the problem of turbulent flame propagation, having a special advantage in that it can be used to discover relationships between the rate of reaction and the patterns of the mean flow.

The development of the high-output combustion chamber for jet power plants has aroused considerable interest in turbulent flame propagation in consequence of the joint requirements of high heat-release rate, (British thermal units per hour per cubic foot), and small frontal area for such engines. These requirements mean efficient use of combustion-chamber volume at high feed velocities; the unavoidable result is turbulent flow.

The laminar flame and the well-stirred reactor (*8, 14*) are two cases of flame propagation sufficiently well understood for quantitative treatment by the engineer. As long as the region of interest is not far removed from these extremes, adequate treatments for engineering use can be developed by modification of the quantitative descriptions of the extremes (*7, 9, 11, 20, 29, 32, 36, 38, 39*).

Theoretical discussion of turbulent flame propagation has to a large extent been based on relationships between the character of the flame front and the turbulence parameters of the unburned mixture (*3, 10, 11, 19, 24, 26, 37, 38*). Scurlock (*24, 25, 33*) has pointed out however that velocity gradients caused by combustion of part of the feed can generate turbulence in an initially laminar stream. Such turbulence can affect the combustion of the remainder of the feed, and his data on confined flames (*25, 33*) indicate that it can have a stronger effect on the flame than turbulence produced by flame holders or turbulence of the feed mixture.

Some measurements of over-all reaction rate of both confined and open turbulent flames have been made (*4, 28, 40*), and Petrein et al. (*18*) have reported measurements of combustion efficiency as a function of longitudinal position for confined flames. Calculations of burning velocity and reaction time at several positions within confined flames have been made by Archer (*1A*), Jacobi (*1B*), and Schilly (*21A*) [see also *37*] from measurements of composition, impact and static pressures, and flame luminosity. Their results indicate a complex interplay of flame and flow.

The complexities shown by the work cited indicate that a more detailed treatment of the turbulent burning zone than attempted heretofore is required. It was the purpose of the work described herein to attempt determniation of reaction rates as a function of position within the flame by means of sufficiently detailed mapping of the composition and velocity patterns.

For purposes of the present discussion the rate of production of any species, j, will be defined as the net efflux of j from any elemental volume of the system when the efflux is considered in terms of the time-mean variables of the system only. Thus the equation of continuity for species j may be written

$$\rho\vec{u}\cdot\nabla\chi_j - \nabla\cdot\xi\nabla\chi_j = Q_j \qquad (1)$$

where the first term on the left is the mass flux, the second term is the diffusive flux, and all quantities are time-mean values. It has been assumed in writing Equation (1) that the coefficient of turbulent diffusion is independent of direction and that molecular diffusion is negligible. Neglect of molecular diffusion allows one to use mass fraction as the composition variable, eliminating the necessity for treatment of mass linear velocity and mole linear velocity in the same expression; χ_j is the mass fraction of j.

If one assumes for the moment that the eddy diffusivity is a known quantity, the quantities required for calculation of Q_j are the velocity components, the density, and the mass fraction of the component in question as functions of position within the flame. The simplest measurements from which to obtain these data are impact pressure, static pressure, and gas composition. A measurement of the temperature is difficult in a flame, and it was decided to calculate the density from the gas composition by assuming that the system is adiabatic, that molecular transport of energy is negligible, and that turbulent heat conduction cannot be distinguished from its associated transfer of mass. Thus since changes in kinetic energy of the flowing gases were always small, the density could be determined by the composition alone; that is, the energy equation becomes

$$H = \text{constant}$$

Since impact pressure is dependent on the square of the velocity, there is no procedure in the absence of knowledge of the turbulence intensity for deducing the true time-mean velocity from measurements of impact and static pressures. In the interest of expediency it was decided to ignore the difference between the velocity determined from these two measurements and the true time-mean velocity.

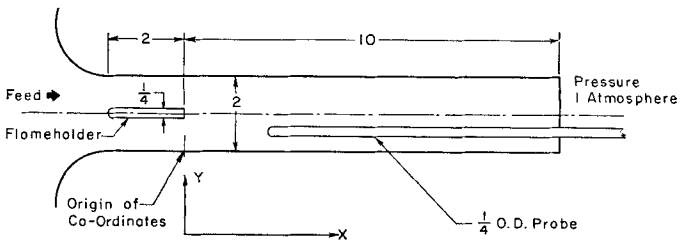

Fig. 1. Atmospheric burner mixture: stoichiometric propane-air, entrance velocity 60 ft./sec.

R. P. Barbor is with the Sun Oil Company, Marcus Hook, Pennsylvania; J. D. Larkin with Monsanto Chemical Company, Springfield, Massachusetts; H. E. von Rosenberg with Humble Oil and Refining Company, Baytown, Texas; and C. W. Shipman with Worcester Polytechnic Institute, Worcester, Massachusetts.

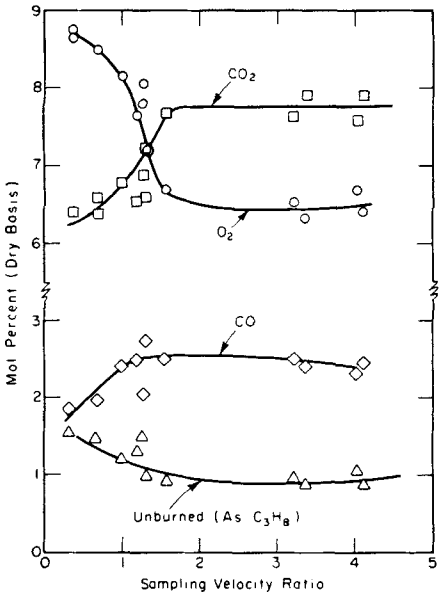

Fig. 2. Effect of sampling rate on sample composition.

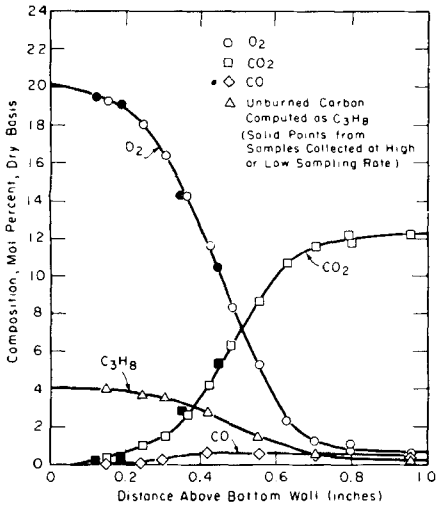

Fig. 3. Gas compositions 8 in. from flame holder. Exhaust pressure 1 atm. Inlet velocity 60 ft./sec., stoichiometric propane-air.

EXPERIMENTAL

It was decided to attempt some measurements of reaction rate in a simulated ramjet combustor. In such burners the flame is first subjected to a flow pattern owing primarily to the flame holder or pilot and in a secondary way to the approach flow; as the combustion proceeds, the flow pattern is altered by velocity gradients generated by the flame itself; finally, as the flame propagates to the confining walls, the geometry of the duct becomes important. It was thought that if the measurements of reaction rate could be made with some success in such a system, the feasibility of this method of attack would be established.

Two experimental arrangements were available at the University of Delaware Combustion Laboratory, both constructed under the supervision of Kurt Wohl. A detailed report of the work on one burner follows, and a summary of the results from the other is given at the end of the discussion. Complete descriptions of both combustors may be found (*1, 22, 30*).

The atmospheric combustion chamber is shown schematically in Figure 1. The feed stream of homogeneously mixed propane and air was introduced into the 2- by 1½- by 12-in. duct through a plenum chamber and nozzle to ensure a flat entrance velocity profile and an initial turbulence level of less than 0.5% (*22*, 30). The exit of the chamber was open to the atmosphere. The flame holder was a flat plate, ¼ in. thick, 2 in. long, and 1½ in. wide, aligned with its long (2 in.) dimension parallel to the flow. The leading edge was rounded to form a semicylinder. The origin of the coordinate system used in later discussion is shown in Figure 1.

For the experiments described herein the inlet velocity varied from 59 to 61 ft./sec., and the feed composition varied from 4.01 to 4.06 mole % propane. Measurements of composition, impact pressure, and static pressure were made at approximately 0.05-in. intervals in the direction normal to the bulk flow (y direction or transverse direction) and at distances of 2, 3, 4, 5, 6, 8, and 10 in. from the downstream end of the flame holder (x or longitudinal positions). Measurements were confined to half the chamber, symmetry and two-dimensionality of the mean flow being assumed.

The probe for measuring impact pressure and withdrawing samples was 20 in. long, 0.25 in. O.D., and 0.04 in. I.D. The tip of the probe was hemispherical in shape. When the probe was employed for withdrawing samples, the pressure drop through the probe was used to measure the sampling rate, the probe having been calibrated for this purpose. The probe used for measurement of static pressure was similar, except that the 0.04 in. pressure-tap hole was located 0.72 in. from the tip and oriented so that the normal to the hole was parallel to the 1½ in. dimension of the combustor. Both probes were inserted into the chamber from the downstream end. No attempt was made to correct measurements of probe position for variations in effective stagnation point due to velocity and density gradients because quantitative methods for making the latter correction are not available. Schlieren photographs and visual observations gave no indication that the character of the flame was altered by the presence of the probe at longitudinal distances greater than 2 in.

Analyses of gas samples were made by the Orsat technique, carbon dioxide being obtained by absorption in 28% (by weight) potassium hydroxide, O_2 by absorption in Oxsorbent, carbon monoxide and H_2 by partial oxidation over copper oxide at 295°C., followed by absorption of the carbon dioxide produced in potassium hydroxide; unburned materials remaining were found by catalytic oxidation with 200% excess oxygen followed by absorption of the carbon dioxide produced in potassium hydroxide and absorption of the excess O_2 in Oxsorbent. Since there is always some uncertainty in Orsat analyses for unburned hydrocarbon, coincidence of the carbon: nitrogen ratio of the sample as analyzed with that of the feed mixture was used as a criterion for the correctness of the analysis in an effort to avoid repeated analyses.

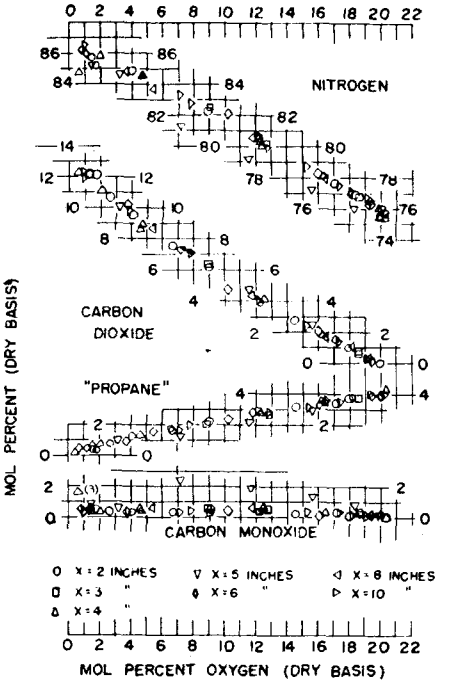

Fig. 4. Composition correlation, 1 atm. flame.

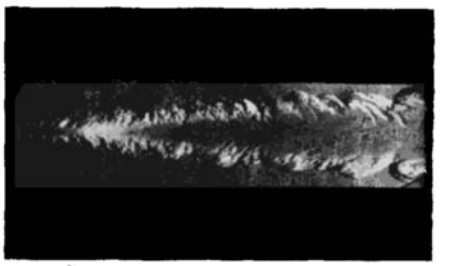

Fig. 5. Schlieren photograph, 1 atm. flame.

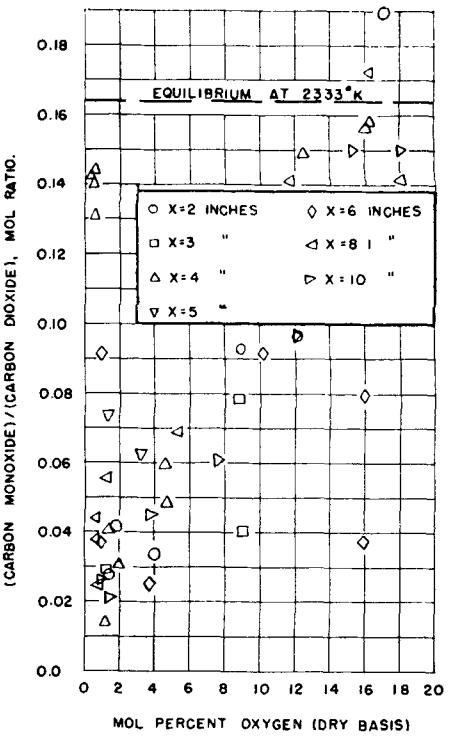

Fig. 6. (Carbon monoxide)/(carbon dioxide) mole ratio, 1 atm. flame.

Tables of Data

60 ft./sec. Atmospheric Propane-Air Flame

Because of nonuniformity in sampling positions and space limitations presentation of all original data is not possible. The following tables show some of the smoothed results. Original data may be found in (*1*) and (*21*)

Table 1. Static Pressures (lb./sq. ft. Gauge)

y	$x = 1$	$x = 2$	$x = 3$	$x = 4$	$x = 5$	$x = 6$	$x = 8$	$x = 10$
0.1	17.53	16.3	14.74	12.88	11.08	9.2	4.95	0.573
0.2	17.42	16.3	14.7	12.7	11.03	9.08	4.76	0.416
0.3	17.22	16.25	14.62	12.6	10.91	9.08	4.89	0.52
0.4	17.04	16.03	14.47	12.5	10.82	9.08	4.89	0.573
0.5	16.9	15.98	14.36	12.55	10.85	9.1	4.89	0.573
0.6	16.9	15.78	14.31	12.7	10.91	9.14	4.89	0.573
0.7	16.9	15.74	14.36	12.75	10.97	9.14	4.89	0.573
0.8	17.07	15.95	14.47	12.75	10.97	9.14	4.89	0.468
0.9	17.28	16.06	14.47	12.75	10.97	9.14	4.89	0.468
1.0	17.48	16.02	14.47	12.8	10.97	9.14	4.89	0.468

Table 2. Velocity (Absolute Value of Total Velocity)

0.1	70	80	89	95	107	123.5	138
0.2	70	80	89	96	108.5	132	163
0.3	70	80	90	100	115	147	175
0.4	70	80	94	112.5	129.5	167	197
0.5	70	82.5	107.5	128	147	187	219
0.6	70	91	122.5	144	165.5	206.5	241.5
0.7	73.5	104.5	137	160	183	226	264
0.8	91	117.5	152	176	201	246	286
0.9	86	131	167	191	219	265	307.5
1.0	84.5	139	174.5	197	228	274	315

Table 3. Densities (lb./cu. ft.)

0	0.0758	0.0757	0.0758	0.0757	0.0753	0.0752	0.075
0.1	0.0758	0.0757	0.0758	0.0757	0.0722	0.0641	0.063
0.2	0.0758	0.0757	0.0758	0.0745	0.0668	0.0485	0.036
0.3	0.0758	0.0757	0.0758	0.0685	0.0507	0.0308	0.0223
0.4	0.0758	0.074	0.071	0.048	0.0317	0.0187	0.0156
0.5	0.0758	0.0658	0.0385	0.024	0.0187	0.0128	0.0113
0.6	0.0743	0.046	0.0207	0.0135	0.0133	0.0103	0.01
0.7	0.0518	0.0213	0.0119	0.0103	0.0102	0.0096	0.0097
0.8	0.0172	0.0113	0.0099	0.0099	0.0096	0.0094	0.0095
0.9	0.010	0.0099	0.0097	0.0097	0.0094	0.0094	0.0094
1.0	0.0097	0.0096	0.0096	0.0095	0.0094	0.0094	0.0094

Table 4. Weight Fraction Burned

0						0.005	0.026
0.1					0.001	0.029	0.070
0.2					0.017	0.087	0.171
0.3				0.017	0.07	0.217	0.326
0.4			0.012	0.083	0.208	0.408	0.535
0.5		0.001	0.086	0.265	0.438	0.643	0.738
0.6		0.06	0.317	0.556	0.707	0.834	0.879
0.7	0.021	0.348	0.677	0.825	0.885	0.924	0.935
0.8	0.359	0.795	0.901	0.929	0.943	0.954	0.957
0.9	0.894	0.934	0.947	0.953	0.959	0.963	0.963
1.0	0.936	0.944	0.95	0.955	0.959	0.963	0.963

It was discovered at the outset that there is a significant effect of rate of sample withdrawal on the composition of the sample obtained. This is illustrated in Figure 2, where the mole percentages of O_2, carbon dioxide, carbon monoxide, and unburned material (calculated as the average of the propane equivalent to the carbon dioxide and to the water produced by the catalytic oxidation) on a dry basis are plotted against the ratio of sampling velocity to stream velocity. The analytical techniques were in a process of evolution at the time these data were taken, and the precision is poorer than obtained in later work. The carbon monoxide fraction is higher than reported in the final data because the fractional combustion was carried out at 320°C., and probably part of the unburned hydrocarbon was also oxidized. However the influence of sampling rate is unmistakable.

It is believed that the variation in sample composition with sampling rate is a consequence of sampling an unmixed stream of varying density; that is, the reaction zone is not homogeneous. This problem has been examined by Leeper (*12*) and Muhlbauer (*16*). Simple theory indicates that variations in density cause variations in pressure at the tip of the sampling probe, when the velocity at the probe tip is different from the stream velocity. Generally if the sampling velocity is less than the stream velocity, higher density material will be sampled preferentially, *et contra*. This simple theory seems to be borne out by the data shown in Figure 2. Theory and experiment (*12*) indicate that samples withdrawn at the velocity of the stream will contain the correct proportions of high- and low-density material.

It might at first be supposed that the increased fraction of burned gases with increasing sampling velocity is a consequence of increased time required for quenching the gases sampled at higher velocity. Application of the available heat transfer correlations (*15*) shows that the time required for cooling the sampled gases is independent of sampling velocity.

Thus it was decided to remove samples at stream velocity. This could be accomplished only if the stream velocity were known, and a trial-and-error procedure was necessary. From an assumed stream density and impact and static pressure measurements, a trial value of the stream velocity was calculated, and a sample was withdrawn at that velocity. From an analysis of this sample a new value of density was computed and the procedure repeated until the assumed and calculated densities agreed within 5%. At those points where concentration gradients were steepest, three or four samples were sometimes required. Figure 3 is a typical set of composition profiles.

The method of calculation of density from an analysis of the sample is important. Since it is impossible to determine by catalytic combustion the exact structure of the unburned material in the sample, and since the effect of sampling rate on sample composition indicates that the reaction zone is inhomogeneous, it was assumed for purposes of density calculation that the material oxidized by catalytic combustion was fuel, and the amount was computed as the average equivalent of the carbon dioxide and water produced by the oxidation. The inhomogeneity of the burning zone is a consequence of rapid chemical reaction rates as opposed to mixing rates, and in the extreme this means that the burning zone consists of completely burned gases and feed mixture. The sample was divided into a burned part, assumed to be at its adiabatic flame temperature, and an unburned part, assumed to be at the temperature of the feed mixture. The reciprocal of the mass-average specific volume of the two parts was used as the mean density of the stream.

For a few cases the density was calculated by assuming homogeneity of the stream. This required extrapolation of the available heat-capacity data for propane. The results were not significantly different from those obtained by the method described above.

Figure 4 is a plot of the experimentally determined mole fractions (dry basis) of nitrogen, carbon dioxide, carbon monoxide, and propane against mole fraction (dry basis) of oxygen. For the sake of clarity some overlapping points have been omitted from this plot. It can be seen that compositions at all longitudinal positions

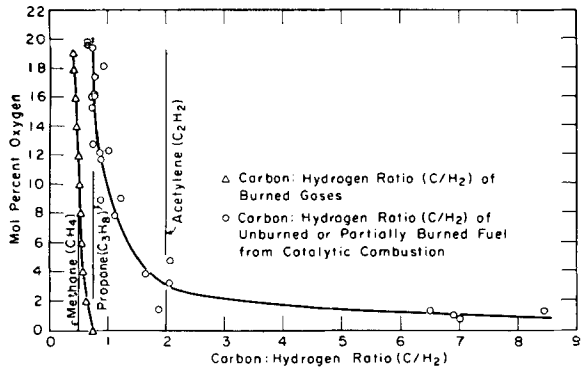

Fig. 7.

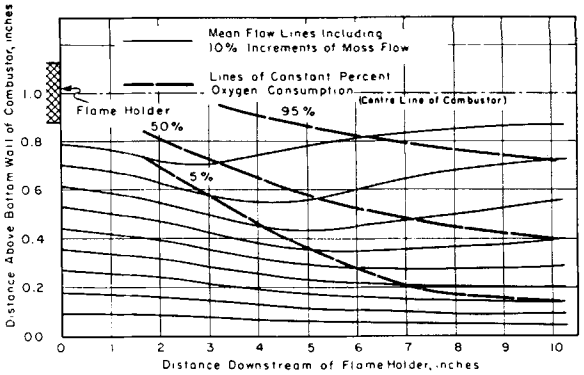

Fig. 9. Lines of mean flow, atmospheric burner.

except $x = 5$ in. can be found within experimental error from a knowledge of carbon dioxide or oxygen content alone. The deviation of the data at $x = 5$ in. for carbon monoxide, propane, and nitrogen is consistent with the possible oxidation of some unburned fuel in the fractional combustion step. The correlation indicated by Figure 4 was used to complete the compositions for $x = 5$ in. from measurements of carbon dioxide and oxygen concentrations. A similar procedure was used for the 3 in. longitudinal position, where insufficient complete analyses were available.

The correlation of Figure 4 was used to reduce the amount of work required to estimate the stream velocity, for the correlation allows estimation of the density from a knowledge of the oxygen concentration. Once sufficient data had been obtained to establish the correlation, a good estimate of the stream density could be obtained by analysis for oxygen alone.

Smoothed results are shown in Tables 1 to 4.

RESULTS AND DISCUSSION

Chemical Structure of the Burning Zone

Examination of the composition traverse in Figure 3 shows the expected behavior of a gradual decrease of unburned species and an increase of burned species as the center of the flame is approached. In addition an increase in breadth of the zone of changing composition with increasing downstream distance was found. In all cases unburned material, that is, that part of the sample burned to carbon dioxide and water upon catalytic combustion with oxygen at 500°C., was found at the center of the flame, usually less than 0.5 mole % (dry basis). The presence of such unburned material is apparently a consequence of the inhomogeneity of the burning zone. and unburned material is thrown into the middle of the flame by the random motion of the gases. Figure 5 is a short-exposure schlieren photograph of the flame, and a few striations near the center of the flame support the conclusion that this region is inhomogeneous. If such striations are present 1.5% of the time at any given longitudinal position, the required amount of unburned material would be accounted for.

It is interesting to note that any hydrogen found in the samples was less than the analytical error except at $x = 5$ in. where the data appear to be unreliable. When one considers only the burned part of the samples, if this material is really completely burned, the carbon monoxide : carbon dioxide ratio should be the equilibrium value. Rough calculations of the equilibrium composition for adiabatic reaction (*23*) indicate that this ratio should be 0.164. The carbon monoxide : carbon dioxide ratios for data of reasonable precision are shown in Figure 6, and it can be seen that the ratios are near or below the equilibrium value, tending to lower values with decreasing oxygen content (increasing fraction burned). This seems to indicate some reaction of carbon monoxide with oxygen as the burned part of the sample is cooled in the probe.

The analyses were carried out in sufficient detail to permit determination or the carbon : net-hydrogen ratio of the unburned material, and by oxygen balance the carbon : hydrogen ratio of the burned part of the sample could be found. Figure 7 shows these carbon : net-hydrogen ratios as a function of the oxygen content of the samples. It appears from this plot that the hydrogen is burned from the hydrocarbon molecule before the carbon and that partial oxidation of the hydrocarbon does take place to some extent. The extermely high carbon : net-hydrogen ratios of the unburned material for low oxygen concentrations are probably the result of poor precision in analysis of small amounts of material. This result bears further study with more reliable analytical techniques.

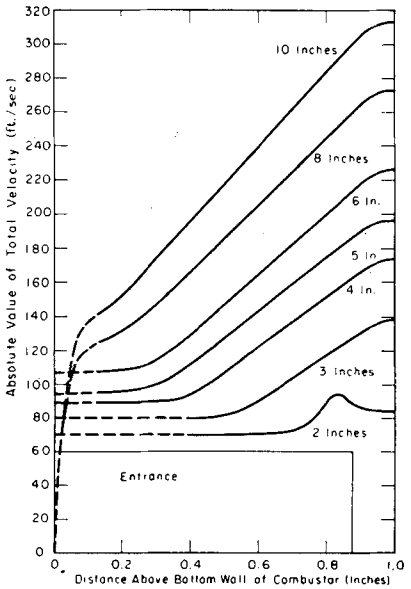

Fig. 8. Velocities calculated from impact pressure, atmospheric burner.

Calculation of Reaction Rates

The quantities required, in addition to the compositions and densities already discussed, are the velocity components. Velocities were determined from measurements of impact and static pressures, and the resulting profiles are shown in Figure 8 with longitudinal position as the parameter. The peculiarly shaped profile for $x = 2$ in. is probably a consequence of the acceleration produced by the reaction in combination with the low velocity downstream of the flame holder; the other profiles show a consistent increase of velocity and velocity gradient with increasing distance downstream from the flame holder.

Some evaluation of the accuracy of the velocity data must be made. The only physical principle which can be used for such an evaluation is conservation of mass, since the feed rates of fuel and air were metered independently of the measurements within the flame itself. On the assumption that the velocities obtained from the impact measurements are the longitudinal components, evaluation of the data can be made by comparing the integrated-mass flow rates, calculated from the burning-zone data with the metered flow rates. The results are shown in Table 5.

It can readily be seen that on the basis of this comparison the data are reasonably consistent.

As pointed out in connection with the calculation of density from the chemical analyses, it was convenient to divide the

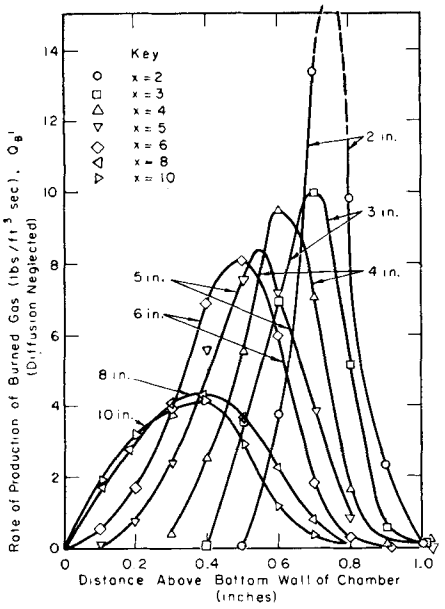

Fig. 10.

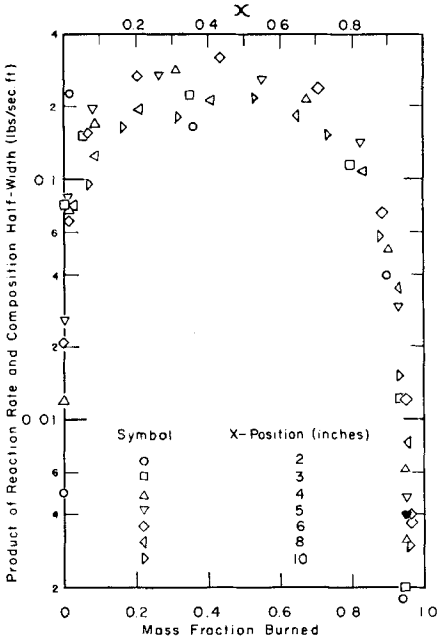

Fig. 11.

TABLE 5—ATMOSPHERIC PROPANE-AIR BURNER

Longitudinal position, in.	One-half the metered mass flow, lb./sec.	Integrated mass flow for one-half the duct, lb./sec.	Error, %
2	0.0414	0.0428	+3.4
3	0.0426	0.0439	+3.1
4	0.0427	0.0442	+3.5
5	0.0425	0.0424	−0.2
6	0.0425	0.0422	−0.7
8	0.0422	0.0411	−2.6
10	0.0421	0.0425	+1.0

samples into burned and unburned parts. This division permitted determination of the mass fraction burned for each sample. It was decided to calculate the rate of generation of burned gas rather than the rate of generation of any particular molecular species. Although detailed treatment of the gas analyses shows that the unburned material is not all propane (Figure 7), the check of mass flow rates indicates that the error in assuming the unburned material to be propane is not great. The correlation of compositions with oxygen concentration (Figure 4) indicates that mass fraction burned is correlated with oxygen content and that the rate of generation of burned gas is nearly proportional to the rate of oxygen consumption.

The results of calculation of rates of generation with turbulent diffusion neglected (or rate of generation plus diffusion) will be presented first. Rewriting Equation (1) yields

$$\rho\vec{u}\cdot\nabla\chi_B = Q_B + \nabla\cdot\xi\nabla\chi_B = Q_B' \quad (2)$$

The left-hand side can be calculated without knowledge of the turbulent diffusion coefficient. The evaluation of the density and mass fraction burned from the data has already been discussed.

The calculation of the two velocity components was carried out as follows. First it was assumed that the impact pressure was owing to the longitudinal velocity component alone. Lines of constant $\int_0^y \rho u_x\, dy$ were plotted on y vs. x coordinates, the direction of the lines at any point being the direction of the mean velocity vector. Some of the mean flow lines are shown in Figure 9 together with lines of 5, 50, and 95% oxygen consumption, an indication of the spreading of the reaction zone. The general character of the mean flow pattern is similar to that calculated by Scurlock (*25, 33*), although the quantitative details are necessarily different. Second, the slopes of the mean flow lines ($\tan\alpha$) were found by the Douglass-Avakian method (*27*), which involves fitting the quartic equation having the least squared error to seven equally spaced points and finding the derivative of the resulting equation, at the central point where possible. The velocity components were then computed from the equation

$$u_y = u_x \tan\alpha \quad (3)$$

The impact pressure is insensitive to direction of the probe axis for angles between probe axis and velocity vector of less than 6 deg. The largest angle between the mean flow lines and the axis of the combustor was 5.5 deg., and while this indicates that the impact pressure was a measure of the absolute value of the total velocity, the cosine of 5.5 deg. is 0.9954 and $u_x = |\vec{u}|$ within an accuracy of 0.5% for the worst case. Thus it was not considered necessary to modify the results obtained as previously described.

The partial derivatives $\partial\chi_B/\partial x$ and $\partial\chi_B/\partial y$ were found by the Douglass-Avakian method (*27*) from tabulations of χ_B at x intervals of 1 in. and y intervals of 0.05 in. The values of χ_B were taken from smooth curves through the data.

Figure 10 shows the calculated values Q_B' as functions of the distance above the bottom wall of the chamber with longitudinal position as a parameter. The increased thickness of the reaction zone with increased distance from the flame holder is not surprising, as this corresponds to the pattern of the luminosity and the schlieren image. It is perhaps more surprising that the maximum value of the volumetric reaction rate decreases with increasing downstream distance. If this is real and not a consequence of failure to account for turbulent diffusion, it might be explained by a rather simple model. One might suppose that the reaction takes place at the periphery of parcels of unburned gas, that the flame surrounding each parcel is laminar, and that the rate of burning is the laminar burning velocity, the effect of variations in flame-front curva-

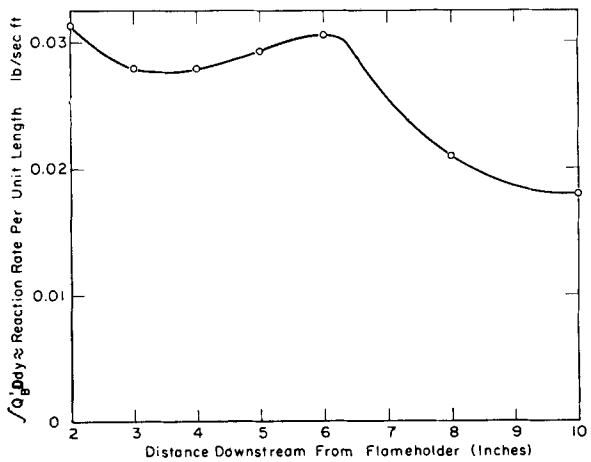

Fig. 12. Reaction rate per unit length (diffusion negligible).

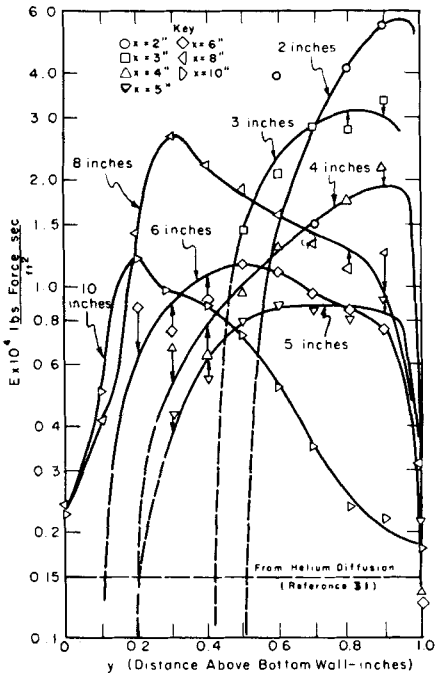

Fig. 13. Eddy viscosities.

ture being neglected. For a given mean composition (fraction burned) the size of the parcels of unburned gas may be visualized as proportional to the scale of the turbulence. Assuming that the parcels are, on the average, spherical, one may write

$$m = \frac{4}{3}\pi\left(\frac{l}{2}\right)^3 n\rho_u \qquad (4)$$

The area of the parcels may be written $\pi l^2 n$, and the reaction rate per unit volume is

$$Q_B = \rho_u S_L \pi l^2 n = \frac{6 S_L m}{l} \qquad (5)$$

Thus it might be expected on the basis of this simplified model that the product $Q_B l$ is a function of the mean composition. If one assumes further that the scale of turbulence is proportional to the composition half-width of the reaction zone (the schlieren image shows increasing scale of wrinkles with increased spreading of the flame), the relationship suggested by Equation (5) may be tested by plotting the product of Q_B' and the value $(1 - y)/12$, with y chosen to correspond to the point at which $\chi_B = (1/2)\chi_{BCL}$, against mass fraction burned. Figure 11 is such a plot, semilogarithmic coordinates being used to spread low values of the ordinate. (It should be noted that a similar relationship could be obtained using the wrinkled flame model.) While the correlation is not impressive, it does illustrate a useful result of this method of attack on the problem of turbulent flame propagation. The correlation could probably be improved by taking cognizance of other flow-pattern parameters (for example, velocity gradient), but in view of the paucity of data more complicated correlations were not attempted. It should be noted that for engineering purposes a correlation which allows prediction of Q_B' is as useful as a set of correlations for Q_B and ξ.

A necessary (but not sufficient) condition on the values of Q_B' is that the over-all reaction rate for the combustor

$$\int_0^{0.833}\left[\int_0^{0.0833} Q_B'\, dy\right] dx$$

be equal to the rate at which burned material leaves the burner

$$\left[\int_0^{0.0833} \rho u_x \chi_B\, dy\right]_{x=0.833}$$

It was found that these quantities agreed within 5%. This comparison is valid because the longitudinal diffusion is small.

The over-all reaction rates per unit length at various longitudinal positions have been compared in Figure 12, and it can be seen that the over-all reaction rate per unit length is relatively constant except for a decrease near the combustor exhaust, where the flame has nearly reached the wall. The data of Petrein et al. (*18*) show similar behavior.

Next the problem of proper allowance for turbulent diffusion is considered. (In terms of gradients of mean composition neglect of molecular diffusion is justified.) The only published data on turbulent diffusion in flames of this sort known to the authors are those of Westenberg (*31*). These data consist of measurements of mean displacement of helium injected into the flame as a function of distance downstream from the injection point and velocity of the gas stream in the region of interest. Data were corrected for molecular diffusion. By means of the Einstein equation

$$\overline{d^2} = 2\xi\theta \qquad (6)$$

a turbulent diffusion coefficient can be calculated. The values thus obtained are so low that the turbulent-diffusion term is negligible in comparison with Q_B'.

Owing to the fact that Westenberg's data were obtained from a burner of a different configuration and his published measurements confined to the center of the duct (Westenberg reports that measurements at other points gave similar results), it was decided to attempt calculation of the eddy viscosity from the present data and to estimate the eddy diffusivity by assuming a turbulent Schmidt number of unity.

$$\frac{E g_c}{\xi} = 1 \qquad (7)$$

There remains the problem of an adequate definition of eddy viscosity for the case at hand. The definition chosen is given by writing the momentum equation as

$$-\nabla p + 2(\nabla \cdot E \nabla)\vec{u} + \nabla \times [E(\nabla \times \vec{u})] = \frac{1}{g_c}[(\rho\vec{u}\cdot\nabla)\vec{u}] \qquad (8)$$

As in writing Equation (1), molecular transport has been neglected, and E has been assumed to be independent of direction. This definition assumes proportionality between stress owing to turbulent transport and rate of strain. It will be noted that Equation (8) is not analogous to the equations of Navier-Stokes in two respects: (1) the static pressure is not defined as the arithmetic average of the normal stresses owing to turbulence, and (2) allowance has been made for variation of transport coefficient with position.

Of the three components of Equation

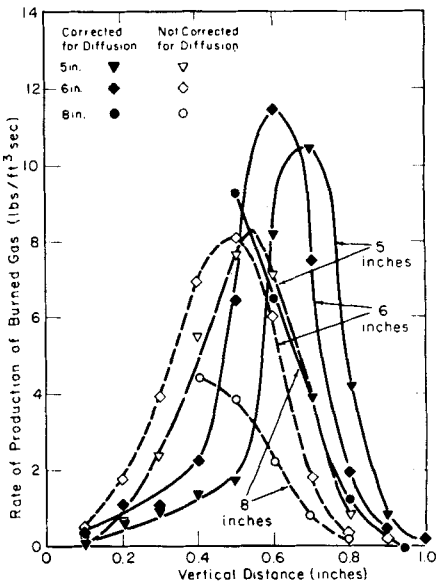

Fig. 14. Effect of turbulent diffusion on calculated reaction rates.

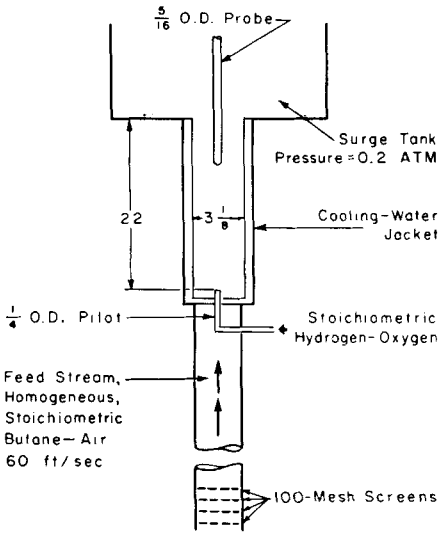

Fig. 15. Low-pressure burner.

(8) the longitudinal (x) component was chosen for finding eddy viscosities because it could be evaluated more accurately, and the x component of the stress is, in the present case, primarily due to mass transport in the y direction; examination of the composition gradients shows that it is this transport which is most important in calculating the reaction rates.

The longitudinal component of the momentum equation is, in cartesian coordinates,

$$-\frac{\partial p}{\partial x} + E\left[2\frac{\partial^2 u_x}{\partial x^2} + \frac{\partial^2 u_x}{\partial y^2} + \frac{\partial^2 u_y}{\partial x\,\partial y}\right] + 2\left(\frac{\partial E}{\partial x}\right)\left(\frac{\partial u_x}{\partial x}\right) + \frac{\partial E}{\partial y}\left(\frac{\partial u_x}{\partial y} + \frac{\partial u_y}{\partial x}\right) = \frac{1}{g_c}\left[\rho u_x \frac{\partial u_x}{\partial x} + \rho u_y \frac{\partial u_x}{\partial y}\right] \quad (9)$$

The longitudinal gradient of the static pressure was obtained by fitting a cubic equation to the data and finding the derivatives of the cubic at the points of interest. Since static-pressure data were available at longitudinal positions 1, 2, 3, 4, 5, 6, 8, and 10 in. downstream from the flame holder, the procedure was found to give reasonable results at all positions reported except at $x = 10$ in. For the evaluation at the 10-in. position it was assumed that the static pressure at distances greater than 10 in. downstream from the flame holder was 1 atm., and the Douglass-Avakian method (*27*) was used to obtain the derivatives. The velocity derivatives were obtained at 0.05-in. y intervals by the Douglass-Avakian method. Second derivatives were calculated by the same method from smoothed curves through the first derivatives.

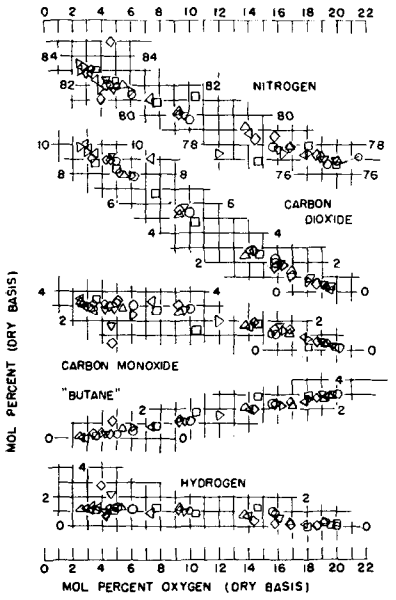

Fig. 16. Composition correlation, 0.2 atm. flame.

In the calculation of E from Equation (9) it was found that the term $\partial E/\partial x$ had a relatively small influence and could be neglected as a first approximation. This permitted rewriting Equation (9) as a total differential equation in the form

$$\frac{dE}{dy} + \frac{E}{g(y)} = \frac{f(y)}{g(y)} \quad (10)$$

Equation (10) can be integrated directly to give

$$E_2 \exp\left[\int_0^{y_2} \frac{dy}{g(y)}\right] - E_1 \exp\left[\int_0^{y_1} \frac{dy}{g(y)}\right] = \int_1^2 \frac{f(y)}{g(y)}\left[\exp\left(\int_0^{y} \frac{dy}{g(y)}\right)\right] dy \quad (11)$$

This equation was then used to calculate E by graphical integration of the separate terms. It is of course necessary that one value of E be known. By symmetry $E = f(y)$ at the center line, but unfortunately the integrand on the right is indeterminate at that point. For the 8- and 10-in. positions it was found that the values of E were relatively insensitive to various extrapolations of the integral on the right, and the centerline values of E were used. For all other positions it was assumed that $E = 0$ in the region where the velocity was practically independent of y, giving another fixed value.

The results of the calculations are shown in Figure 13, where the calculated points are shown. A value of the eddy viscosity calculated from Westenberg's data (*31*) by use of Equations (6) and (7) is also shown.

In spite of the apparent confusion of the curves they do follow a reasonable pattern. There are in the system studied three sources of velocity gradients which could result in turbulence and consequently in appreciable values of eddy viscosity.

1. Velocity gradients caused by the flame holder. Turbulence from this source would be expected to spread and to die out with increasing distance from the flame holder. The high values of eddy viscosity near the center of the duct which decrease with increasing values of x are apparently due to this source. The flame holder used for this study probably has a greater influence on the flow than the flame holders in general use, owing to its length, which causes appreciable boundary-layer build up, and to its bluff nose, which probably causes a bow wave.

2. Velocity gradients caused by the combustion process itself. As already pointed out, this is a major source of flame-generated turbulence in confined flames. This source of turbulence accounts for increasing values of eddy viscosity in the region $5 < x < 8$; $0.2 < y < 0.6$.

3. Velocity gradients at the wall. As the boundary layer at the wall increases in thickness, turbulence from this source would be expected to have an increasing influence. In this case its influence appears in the region $6 < x < 10$; $0 < y < 0.2$.

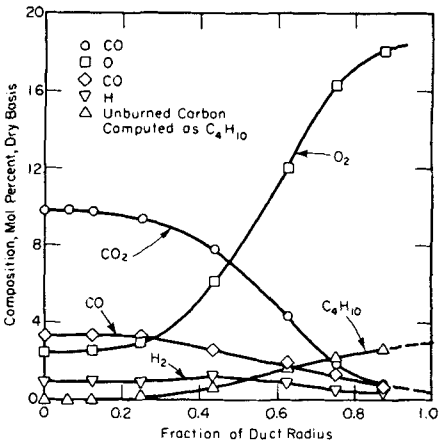

Fig. 17. Gas composition 16 in. from pilot, exhaust pressure 0.2 atm.

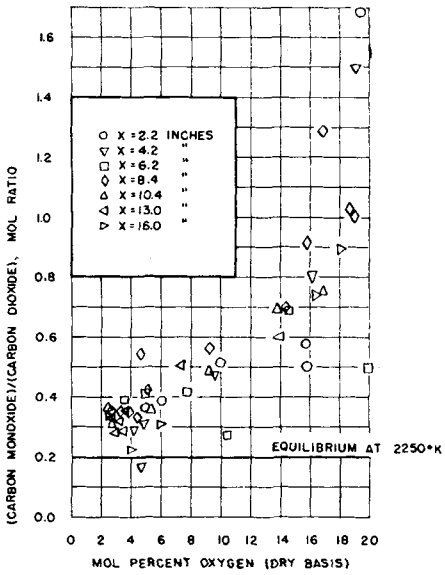

Fig. 18. (Carbon monoxide)/(carbon dioxide) mole ratio, 0.2 atm. flame.

As shown by the dotted horizontal line in Figure 13, the values obtained agree reasonably well with those obtained from Westenberg's data at the center line. Values reported for the 2- and 10-in. positions are inaccurate because these positions are the terminal points of the data and the derivatives are not well defined.

The smooth curves of Figure 13 were used to calculate eddy diffusivities by means of Equation (7). The necessary derivatives again being obtained by the Douglass-Avakian method (*27*), the results were applied to calculation of reaction rates by means of Equation (1). In the region where the flame itself is thought to be the chief source of turbulence, reasonable values of reaction rate were obtained, and these values together with the corresponding results

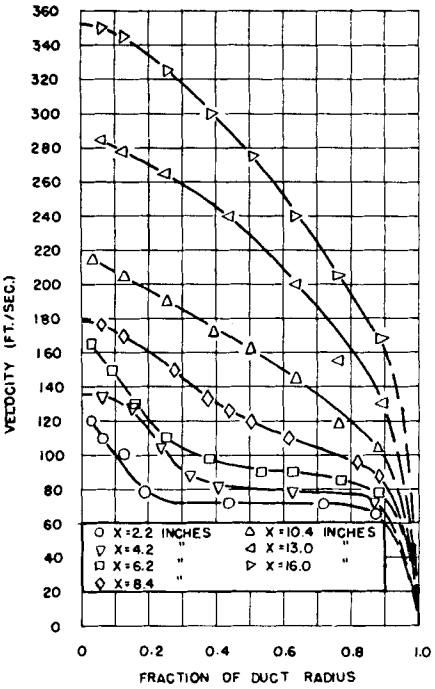

Fig. 19. Velocity profiles—0.2 atm. burner.

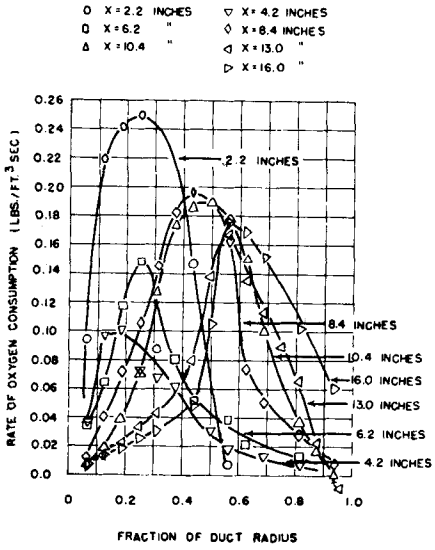

Fig. 20. Rates of oxygen consumption, 0.2 atm. flame.

obtained by neglecting turbulent diffusion are shown in Figure 14. It is obvious that on the basis of these calculations allowance for diffusion is very important, but the results are too meager for generalization. The maximum reaction rate corresponds to a heat release rate of about 50×10^6 B.t.u./(hr.)(cu. ft.).

In the region where the chief source of turbulence is thought to be velocity gradients at the flame holder or the combustion-chamber wall, and where $\nabla^2\chi_B$ is positive, it was found that with few exceptions application of the curves of Figure 13 with Equations (7) and (1) gave negative values of Q_B. Such a result is of course untenable. The coincidence of negative values and source of turbulence together with the consistency of negative values seems to eliminate random errors in computation as the source of the difficulty. It seems rather that the fault lies with the value of the turbulent Schmidt number and that a value greater than unity should be used. While studies of turbulent mass and momentum transport (*5*) have yielded values of the turbulent Schmidt number between 0.63 and 0.74, in most such studies the initial velocity gradient responsible for the turbulence was exactly correlated with the initial composition gradient causing the mass transfer. Furthermore the systems studied were of nearly constant density. While the introduction of a significant density variation alone may affect the turbulent Schmidt number, this is apparently not sufficient to give ridiculous values in that region of the flame where the turbulence is generated by the combustion process and velocity and composition gradients are related. However where gradients of velocity at the wall or flame holder are the predominate source of turbulence, the composition gradient is introduced by the reaction after the generation of turbulence. It may be that most of the reaction takes place in a particular part of the turbulence spectrum. At any rate it is believed that this difference is sufficient to admit the explanation for negative reaction rates in terms of Schmidt numbers greater than unity, but no mechanism can be offered at this time. Numerical values of reaction rates (Q_B'), eddy viscosities and the sample compositions are given in Tables 7, 8, and 9.*

THE 0.2-ATM. SYSTEM

Figure 15 schematically shows the apparatus. The cylindrical combustion chamber was made of Vycor glass. The cold-gas velocity through the pilot tube was 50 ft./sec. Experimental techniques and methods of treating the data were similar to those already described with two exceptions: (1) no provision was made for control of sampling rate and (2) in the analysis of unburned hydrocarbon only the carbon dioxide produced by catalytic combustion was measured.

Figure 16 shows the composition correlation, and a typical set of composition profiles is shown in Figure 17. The scattering of the data points in Figure 16 is probably a result of lack of control of sampling rate. It should be pointed out that while variations in sampling rate affect the relative portions of high- and low-density material, the chemical composition of the two parts is not altered.

The amounts of carbon monoxide and hydrogen found in samples from this flame are significant. A comparison of the carbon monoxide : carbon dioxide ratios of the samples with the equilibrium ratio calculated for adiabatic reaction is shown in Figure 18. While the departure from equilibrium is not great, the reasons for it may be important, especially in view of the results found for the atmospheric flame (Figure 6). The presence of carbon monoxide in excess of the equilibrium amount may be due to (1) quenching of partially burned material in the sampling probe, (2) quenching of small elements of flame by the action of turbulence as shown experimentally by Olsen and Gayhart (*17*), or (3) separation of fuel and oxidant by preferential molecular diffusion of the latter to burning zones within the turbulent flame brush as suggested by Wohl and Shore (*38*) to account for the excessively high-turbulent burning velocity of rich butane-air mixtures. In the latter case the physical picture of a small part of the flame is similar to the patterns obtaining at the edge of the wake of a bluff-body flame holder, and the existence of preferential diffusion in such cases has been demonstrated by Williams and Shipman (*34*), Williams, Woo, and Shipman (*35*), and Zukoski and Marble (*41*).

Figure 19 shows the velocity profiles. Table 6 shows clearly the effect of lack of control of the sampling rate. Qualitative estimates indicated that the sampling velocity was always lower than the stream velocity, and this is supported by the results. Figure 20 shows the rates of oxygen consumption calculated by neglecting diffusion. Obviously these results are at best subject to qualitative interpretation only. The high initial reaction rates are undoubtedly a consequence of the action of the pilot. The subsequent decrease in reaction rates with increasing downstream distance is probably due to dissipation of the pilot stream by turbulence, and the increase in reaction rates at the farthest downstream positions may be attributed to increased velocity gradients and a consequent increase in turbulence intensity. This latter situation was not observed in the atmospheric data because the combustor was too short.

TABLE 6. THE 0.2 ATM. BUTANE-AIR FLAME

Distance downstream from pilot, in.	Metered mass flow, lb./sec.	Integrated mass flow, lb./sec.	% Error
2.2	0.04941	0.0566	+14.55
4.2	0.04941	0.0561	+13.55
6.2	0.04941	0.0575	+16.4
8.4	0.04941	0.0574	+16.2
10.4	0.04941	0.0553	+11.95
13.0	0.04941	0.0600	+21.5
16.0	0.04941	0.0614	+24.3

*Tabular material has been deposited as document 5823 with the American Documentation Institute, Photoduplication Service, Library of Congress, Washington 25, D. C., and may be obtained for $1.25 for photoprints or $1.25 for 35-mm microfilm.

CONCLUSIONS

The analyses of samples from the reaction zone of the atmospheric, propane-air flame show that the composition can be characterized by oxygen concentration only, an indication that the reaction rate can be satisfactorily represented by the rate of oxygen consumption. Results for the low-pressure flame are similar, but the conclusion is less firm because of the effect of lack of control of the samlping rate.

Since the carbon monoxide : carbon dioxide ratios of the samples from the atmospheric flame are less than those corresponding to equilibrium, it appears that there is some reaction in the sampling probe. Since there is an effect of pressure on the composition of the burned gas beyond that expected from equilibrium considerations, it is concluded that there is quenching of flame elements either in the sampling probe or within the turbulent flame itself; preferential diffusion of oxidant from unburned parcels to burning zones within the flame is also considered a possible explanation.

The calculation of reaction rates is hampered by inadequate knowledge of eddy diffusion. While calculations of eddy diffusivity from data in the literature indicate that the effect is negligible, estimates from the present data based on analogy of mass and momentum transfer indicate that turbulent mass transfer is significant. These same estimates, applied to regions where shear at the wall of the combustor or the flame holder is believed to be the chief source of turbulence, gave negative reaction rates. It is concluded therefore that the turbulent Schmidt number is dependent on the relationship between the shear causing turbulence and the introduction of the composition gradient causing mass transfer and possibly on the density patterns.

It was found that the calculated reaction rates are a function of position within the flame as well as of fractional completion of combusition. The data indicate that the reaction rates obtained by neglecting turbulent diffusion are a result of competition between increased turbulence generated by increased velocity gradients and increased scale of turbulence, the former increasing and the latter decreasing apparent reaction rates.

Finally the importance of taking samples from the inhomogeneous reaction zone of a turbulent flame in such a way as to prevent preferential sampling of low- or high-density material cannot be overemphasized. The unsatisfactory results obtained from the 0.2-atm., butane-air flame seem to be directly related to errors of this type.

While neither of the flames studied is in the range of practical, high-output combustor operation, the results show that the method of attack employed is profitable. This is especially so because it affords direct study of relationships between flow patterns, rates of reaction, and general character of combustion products. The work involved in future studies of this kind has been materially reduced by the finding of suitable computational techniques, and the chemical, analytical work may be greatly reduced by use of gas chromatography in conjunction with an oxygen analyzer (dependent on the paramagnetism of oxygen).

From the theoretical viewpoint the method may seem less attractive than those studies involving interaction between a flame and a stream of known turbulence characteristics, but the effect of even unconfined flames on the flow pattern of the feed mixture is too often neglected. It should be pointed out that the same techniques used for the measurement of reaction rates might be used for the study of turbulent mass transfer. The measurement of a coefficient of turbulent diffusion by this method is basically no different from that used in the studies of heat and mass transfer between phases, where systematic measurements have produced results of great utility.

ACKNOWLEDGMENT

The work described herein was done at the University of Delaware under the sponsorship of Project SQUID, which is supported by the Office of Naval Research under Contract N6-ori-105, T.O. III, NR-098-038. The authors express their appreciation to Kurt Wohl for his kind cooperation and encouragement in preparing the work for publication and for his helpful criticism of it. The suggestions and comments of G. C. Williams are also gratefully acknowledged.

NOTATION

D = depth of combustor, normal to xy plane
$\overline{d^2}$ = mean square displacement of injected helium
E = eddy viscosity, (lb.-force)(sec.)/sq. ft.
$f(y)$ = function of y [cf. Equations (9) and (10)]
$g(y)$ = function of y [cf. Equations (9) and (10)]
g_c = conversion constant, (lb.-mass)(ft.)/(lb.-force)(sec.^{2})
H = enthalpy.
l = scale of turbulence or size of unburned parcels
m = mass of unburned gas per unit volume
n = number of unburned parcels per unit volume
p = static pressure
Q = rate of generation of subscript component, lb.-mass/(cu. ft.)(sec.)
Q_B' = rate of generation of burned gas plus diffusion rate
S_L = laminar burning velocity
$\vec{u}$ = velocity vector, $|\vec{u}|$ absolute value of velocity
u_x = longitudinal velocity component
u_y = transverse velocity component
x = longitudinal position
y = transverse position

Greek Letters

α = angle between mean flow line and longitudinal coordinate
θ = time
ξ = coefficient of turbulent diffusion (lb. mass/(sec.)(ft.)
ρ = density
ρ_u = density of unburned gas
χ = mass fraction of subscript component
∇ = vector operator, $(\vec{i}(\partial/\partial x) + \vec{j}(\partial/\partial y) + (\partial/\vec{k}\partial z))$ in Cartesian coordinates

Subscripts

B = burned gas
CL = center-line position

LITERATURE CITED

1. Barbor, R. P., and J. D. Larkin, M.Ch.E. thesis, Univ. Delaware, Newark (1954).
1A. Archer, D. H., Ph.D. thesis, Univ. Delaware, Newark (1953).
1B. Jacobi, W. M., M.Ch.E. thesis, Univ. Delaware, Newark (1953).
2. Berl, W. G., J. L. Rice, and P. Rosen, *Jet Propulsion*, **25**, 341, (1955).
3. Damköhler, Gerhard, *Z. Elektrochem.*, **46**, 601 (1940). English translation: *Natl. Advisory Comm. Aeronaut., Tech. Mem.* 1112 (1947).
4. Fine, B. D., and Paul Wagner, *Natl. Advisory Comm. Aeronaut., Tech. Note* 3277 (June, 1956).
5. Forstall, Walton, Jr., and A. H. Shapiro, *Mass. Inst. Technol. Meteor Rept.* 39 (July, 1949).
6. Fristrom, R. M., and A. A. Westenberg, *Combustion and Flame*, **1**, 217 (1957).
7. Grumer, Joseph, J. M. Singer, J. K. Richmond, and J. R. Oxendine, *Ind. Eng. Chem.*, **49**, 305 (1957).
8. Hottel, H. C., G. C. Williams, and M. L. Baker, "Sixth Symposium (International) on Combustion," p. 398, Reinhold, New York (1957).
9. Hottel, H. C., G. C. Williams, and R. S. Levine, "Fourth Symposium (International) on Combustion," p. 636, Williams and Wilkins, Baltimore (1953).
10. Karlovitz, Bela, "High Speed Aerodynamics and Jet Propulsion," Vol. II, p. 342, Princeton Univ. Press, Princeton, N. J. (1956).
11. Karlovitz, B., D. W. Denniston, Jr., and F. E. Wells, *J. Chem. Phys.*, **19**, 541 (1951).
12. Leeper, C. K., Sc.D. thesis, Mass. Inst. Technol., Cambridge (1954). See also Leeper, C. K., S.M. thesis, Mass. Inst. Technol., Cambridge (1949).
13. Lewis, Bernard, and Guenther von Elbe, "Combustion, Flames, and Explosions of Gases," p. 766, Academic Press, New York (1951).
14. Longwell, J. P., and M. A. Weiss, *Ind. Eng. Chem.*, **47**, 1634 (1955).
Longwell, J. P., "Fifth Symposium (International) on Combustion," p. 48, Reinhold, New York (1955).

15. McAdams, W. H., "Heat Transmission," 3rd ed., p. 238, McGraw-Hill Book Co., New York (1954).
16. Muhlbauer, H. G., M.Ch.E. thesis, Univ. Delaware, Newark (1950).
17. Olsen, H. L., and E. L. Gayhart, *Jet Propulsion*, **25**, 276 (1955).
18. Petrein, R. J., J. P. Longwell, and M. A. Weiss, *ibid.*, **26**, 81 (1956).
19. Richardson, J. M., "Proceedings of the Gas Dynamics Symposium on Aerothermochemistry," p. 169, Northwestern Univ., Evanston, Illinois (1956).
20. Richmond, J. K., J. M. Singer, E. B. Cook, J. R. Oxendine, Joseph Grumer, and D. S. Burgess, "Sixth Symposium (International) on Combustion," p. 303, Reinhold, New York (1957).
21. Rosenberg, H. E., von, Ph.D. thesis, Univ. Delaware, Newark (1955).
21A. Schilly, R. A., M.Ch.E. thesis, Univ. Delaware, Newark (1953).
22. Ries, H. B., Ph.D. thesis, Univ. Delaware, Newark (1951).
23. Rossini, F. D., K. S. Pitzer, R. L. Arnett, Rita M. Braun, G. C. Pimentel, et al., *Am. Petroleum Indust. Res. Proj. 44*, Carnegie Press, Pittsburgh, Pennsylvania (1953).
24. Scurlock, A. C., and J. H. Grover, "Fourth Symposium (International) on Combustion," p. 645, Williams and Wilkins, Baltimore (1953). See also "Selected Combustion Problems, Fundamentals and Aeronautical Applications," p. 215, Butterworths, London (1954).
25. Scurlock, A. C., *Mass. Inst. Technol. Fuels Research Laboratory, Meteor Rept.* 19 (May, 1948).
26. Shelkin, K. I., *J. Tech. Phys. (USSR)*, **13**, 9, 10 (1943). English translation: *Natl. Advisory Comm. Aeronaut., Tech. Mem.* 1110 (1947).
27. Sherwood, T. K., and C. E. Reed, "Applied Mathematics in Chemical Engineering," 1 ed., pp. 287, 266, McGraw-Hill Book Co., New York (1939).
28. Simon, Dorothy M., and Paul Wagner, *Ind. Eng. Chem.*, **48**, 129 (1956).
29. Summerfield, Martin, S. H. Reiter, Victor Kebely, and R. W. Mascolo, *Jet Propulsion*, **25**, 377 (1955).
30. Weil, C. W., Ph.D. thesis, Univ. Delaware, Newark (1950).
31. Westenberg, A. A., *J. Chem. Phys.*, **22**, 814 (1954).
32. Williams, D. T., and L. M. Bollinger, "Third Symposium on Combustion and Flame and Explosion Phenomena," p. 176, Williams and Wilkins, Baltimore (1949).
33. Williams, G. C., H. C. Hottel, and A. C. Scurlock, *ibid.*, p. 21.
34. Williams, G. C., and C. W. Shipman, "Fourth Symposium (International) on Combustion," p. 733, Williams and Wilkins, Baltimore (1953).
35. Williams, G. C., P. T. Woo, and C. W. Shipman, "Sixth Symposium (International) on Combustion," p. 427, Reinhold, New York (1957).
36. Wohl, Kurt, Leon Shore, H. E. von Rosenberg, and C. W. Weil, "Fourth Symposium (International) on Combustion," p. 620, Williams and Wilkins, Baltimore (1953).
37. Wohl, Kurt, "Sixth Symposium (International) on Combustion," p. 333, Reinhold, New York (1957).
38. Wohl, Kurt, and Leon Shore, *Ind. Eng. Chem.*, **47**, 828 (1955).
39. Wright, F. H., *Jet Propulsion Laboratory, Cal. Inst. Tech., Progress Rept. 3-21* (1953).
40. Zelinski, J. J., W. T. Baker, L. J. Mathews, III, and E. C. Bagnall, "Proceedings of the Gas Dynamics Symposium on Aerothermochemistry," p. 179, Northwestern Univ., Evanston, Ill. (1956).
41. Zukoski, E. E., and F. E. Marble, "Combustion Researches and Reviews 1955," p. 167, for AGARD, Butterworths, London (1955).

Manuscript received October 11, 1957; revision received June 19, 1957; paper accepted July 7, 1958.

Low-Temperature Vapor-Liquid Equilibria in Ternary and Quaternary Systems Containing Hydrogen, Nitrogen, Methane, and Ethane

HARRY F. COSWAY and DONALD L. KATZ

University of Michigan, Ann Arbor, Michigan

Experimental data are presented for three ternary systems and the quaternary at pressures of 500 and 1,000 lb./sq. in. abs. and at temperatures of −100° and −200°F. These data along with information in the literature were correlated to give charts of equilibrium ratios as a function of temperature, pressure, and composition.

The compositions of equilibrium vapors and liquids were measured for the quaternary system hydrogen-nitrogen-methane-ethane and three of its ternaries at conditions shown in Table 1. The apparatus and procedures employed were essentially the same as those used by Aroyan, Williams, and Benham (*1*, *12*, *2*). The phase compositions were determined by mass spectrometer.

The experimental data are given in Tables 2 to 5. The binary-system data from the literature are included in the tables at the conditions of the measurements in this research. The following binary-system data were used in correlating the data for the ternary systems: hydrogen-methane (*2*); hydrogen-ethane (*12*), hydrogen-nitrogen (*7*, *9*, *10*, *11*), nitrogen-methane (*5*, *6*), and methane-ethane (*4*). Ternary data for hydrogen-nitrogen-methane (*10*) and hydrogen-methane-ethane (*8*) also were used in correlating the phase behavior of these systems.

For the ternary systems the equilibrium ratios were plotted on three types of cross plots: equilibrium ratios vs. pressure, lines of constant temperature, and charts of constant percentage methane, in the liquid phase; equilibrium ratios vs. temperature, lines of constant percentage methane, and charts of constant pressure; and equilibrium ratio vs. percentage of methane in the liquid,

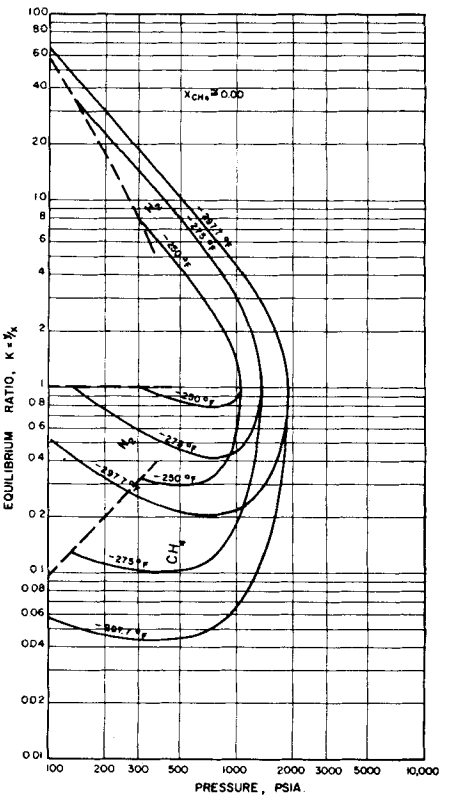

Fig. 1. Equilibrium ratios for constituents in the hydrogen-nitrogen-methane system at 0 mole % methane in the liquid phase as a function of pressure for various temperatures.

Harry F. Cosway is with the American Cyanamid Company, Stamford, Connecticut.